SnowSTNet: A Spatial-Temporal LiDAR Point Cloud Denoising Network for Autonomous Driving in Snowy Weather

Yida Li [1], Xinyuan Yan [1], He Huang [1] Yu Liang [1], Yidan Zhang [1], Junxing Yang [1*]

[1] School of Geomatics and Urban Spatial Informatics, Beijing University of Civil Engineering and Architecture, Beijing, China - yida.li@foxmail.com, yan1075783878@126.com, huanghe@bucea.edu.cn, yu748240@gmail.com, 13212143501@163.com, yangjunxing@bucea.edu.cn

Keywords: autonomous driving, LiDAR, snowy weather, point cloud denoising.

Abstract

Autonomous vehicles perceive their surroundings through sensors such as LiDAR. However, snowflakes are distributed within the detection range of LiDAR sensors in snowy weather, generating noise points that compromise the sensor's detection performance. To mitigate this issue, we propose SnowSTNet, a point cloud denoising network that removes snowflake noise from LiDAR point clouds. In SnowSTNet, we adopt a two-branch network structure that encodes information in both spatial and temporal dimensions, and inputs the features obtained from the spatial branch into the temporal branch as guidance. We conducted comparative experiments on the SnowyKITTI dataset, and the results show that our method significantly outperforms others, achieving an MIoU of 97.19%. The proposed SnowSTNet ensures the reliable operation of self-driving vehicles in snowy weather and promotes the widespread application of autonomous driving technology in complex environments.

1. Introduction

With the rapid development of autonomous driving technology, vehicles have become capable of efficient perception and decision-making in clear weather. However, adverse weather such as snow still pose significant challenges to autonomous driving systems. LiDAR, as a core sensing device in autonomous driving systems, is susceptible to snowflake interference, generating a large number of noise points into the point cloud data. The presence of these noise points degrades data quality, leading to errors in environment perception and path planning, thus threatening vehicle safety. To overcome this challenge, we propose a LiDAR point cloud denoising method designed for snowy weather, which effectively removes snowflake noise while preserving critical environmental features, thereby enhancing the perception accuracy and operational safety of autonomous driving systems.

Denoising methods for point clouds in adverse weather can be broadly divided into two categories: filter-based and deep learning-based methods(Qu et al., 2024). Filter-based denoising methods can be applied to most adverse weather by setting fixed parameters, without the need to train large amounts of point-by-point labeled point cloud data. However, their performance is limited. Deep learning-based denoising methods are the application of neural networks in the field of point cloud denoising. Deep learning techniques were initially applied in point cloud semantic segmentation and later extended to point cloud denoising. Point cloud semantic segmentation is a multi-classification task, whereas point cloud denoising is a binary classification task, a simplification of semantic segmentation. Considering the inherent properties of the noise points, researchers have improved classical semantic segmentation networks, and deep learning-based denoising methods have seen significant advancements in recent years.

Researchers widely use filter-based denoising methods for LiDAR point cloud data. The most classical filters include the Radius Outlier Removal (ROR) filter and the Statistical Outlier Removal (SOR) filter proposed by Rusu et al. (Rusu & Cousins, 2011). Both approaches operate under the assumption that noise points exhibit spatial isolation. ROR operates by quantifying the local point density within a predetermined search radius, designating points as outliers when their neighborhood density falls below an established threshold. In comparison, SOR employs a statistical approach that evaluates the mean K-nearest neighbor distances, subsequently applying a universal distance threshold for outlier identification. Nevertheless, when relying solely on noise isolation characteristics, many authentic environmental features may be erroneously eliminated, resulting in substantial information loss. To address this issue, Charron et al. proposed the Dynamic Radius Outlier Removal (DROR) filter (Charron et al., 2018), improving on ROR by using a dynamic radius to adapt to variations in point cloud density, thereby avoiding misclassification issues caused by a fixed radius in long-range regions. Similarly, Kurup et al. introduced the Dynamic Statistical Outlier Removal (DSOR) filter (Kurup & Bos, 2021), which replaces the fixed global threshold in SOR with a dynamic threshold. Experimental results show that DROR and DSOR can effectively remove most noise points while retaining significant environmental features. In addition to spatial features, researchers have observed that noise points in adverse weather, such as snowy weather, generally have lower intensity values. Based on this observation, Park et al. proposed the Low-Intensity Outlier Removal (LIOR) filter (Park et al., 2020). Building upon the aforementioned classical filters, several improved versions have been developed. Balta et al. proposed the Fast Cluster Statistical Outlier Removal (FCSOR) filter (Balta et al., 2018), which integrates voxel subsampling with the SOR filter. Duan et al. introduced the PCA-based Adaptive Clustering (PCAAC) filter (Duan, Yang, Chen, et al., 2021), which denoises by combining PCA downscaling with adaptive clustering. However, PCAAC performs poorly in long-range sparse regions. To address this limitation, Duan et al. further proposed the PCA-

* Corresponding author

based Adaptive Radius Outlier Removal (PCAAR) filter (Duan, Yang, & Li, 2021), which integrates the Adaptive Radius Outlier Removal (AROR) method, effectively mitigating the impact of point cloud density variations. Roriz et al. proposed the Dynamic Low-Intensity Outlier Removal (DIOR) filter (Roriz et al., 2022), which combines the dynamic radius adjustment of DROR with the intensity thresholding mechanism of LIOR. Wang et al. introduced the Dynamic Distance-Intensity Outlier Removal (DDIOR) filter (Wang et al., 2022), which incorporates both distance and intensity information of the point cloud. Huang et al. proposed the Low-Intensity Dynamic Statistical Outlier Removal (LIDSOR) filter (Huang et al., 2023), which combines distance and intensity thresholds to reduce the risk of false denoising and accelerate processing speed. Finally, Yan et al. developed a denoising framework based on the disordered nature of snowflake noise points, which includes the Time Outlier Removal (TOR) filter (Yan et al., 2024), further enhancing denoising accuracy.

Breakthroughs in neural networks have substantially enhanced the performance of deep learning-based denoising methods. Compared to filter-based methods, deep learning-based approaches can learn higher-dimensional noise features through network architectures, generally outperforming traditional filters. WeatherNet (Heinzler et al., 2020), proposed by Heinzler et al., was the first work to apply convolutional neural networks to point cloud denoising. WeatherNet improves upon the semantic segmentation network LiLaNet (Piewak et al., 2019) by reducing network depth and introducing dilated convolutions and Dropout layers, effectively enhancing denoising performance while reducing computational complexity. Subsequently, SunnyNet (Luo et al., 2022), proposed by Luo et al., further enhanced WeatherNet by incorporating attention modules such as SENet, CBAM, and ECANet, which effectively remove rain and fog noise. Bae et al. proposed a self-supervised learning method called SLiDE(Bae et al., 2022), which removes snow noise points without requiring labeled data. Similarly, Yu et al. introduced LiSnowNet (M.-Y. Yu et al., 2022), an unsupervised snow noise removal algorithm based on the MWCNN network. Building on WeatherNet and SalsaNext (Cortinhal et al., 2020), Seppänen et al. proposed 4DenoiseNet (Seppanen et al., 2023) and created the SnowyKITTI dataset. 4DenoiseNet incorporates temporal features and k-nearest neighbor convolution to significantly improve the removal of snow noise points. Recently, AdverseNet (Yan et al., 2025) has been proposed as a unified denoising network, which effectively removes noise caused by rain, snow, and fog, further improving the quality of point cloud data in complex environments.

This study builds upon 4DenoiseNet, making improvements to address its limitations in temporal and spatial feature fusion. Based on previous research on the distribution characteristics of snowflake noise, we propose a Spatial-Temporal LiDAR Point Cloud Denoising Network for Autonomous Driving in Snowy Weather (SnowSTNet), which uses deep learning techniques to remove snowflake noise. Our method captures the dynamic changes during snowy weather by introducing temporal dimension information and effectively learns the local features of snowflake noise through spatial-temporal kNN-convolution. By analyzing sequential point cloud frames using k-nearest neighbor (kNN), the algorithm effectively exploits temporal correlations, which significantly improves denoising precision. In addition, we incorporate motion-guided attention (MGA) block into multiple network layers to encode information in both spatial and temporal dimensions. The features extracted from the spatial branch are used as guidance for the temporal branch, further optimizing the snowflake noise removal process. The architecture comprises spatial and temporal processing branches, with the former operating on the current point cloud P(t) and the latter analyzing the immediately preceding frame P(t-1). This combination enables the model to more accurately differentiate between noise points caused by snowflakes and environmental features.

The main contributions of this study are as follows:

1) We propose SnowSTNet, a point cloud denoising network based on a two-branch architecture that effectively handles LiDAR noise in snowy weather, thereby enhancing system perception.

2) By utilizing the kNN-convolution operation to extract spatial and temporal features of point clouds, and applying joint encoding through a two-branch architecture with multiple MGA blocks, our method more effectively distinguishes noise points from non-noise points.

2. Methodology

2.1 Data Prepossessing

This study uses a projection-based approach to process LiDAR point cloud data. This method maps the 3D coordinates (x,y,z) of the LiDAR point cloud to a spherical coordinate system and subsequently converts them into a 2D image coordinate system, providing a suitable input format for subsequent convolution operations. First, the 3D coordinates c=(x,y,z) of the LiDAR point cloud are mapped to a spherical coordinate system, then converted to the image coordinate system. The coordinate conversion is performed using the following equations:

$$\begin{bmatrix} u \\ v \end{bmatrix} = \begin{bmatrix} (\frac{1}{2}(1-\tan^{-1}(\frac{y}{x})\cdot\pi^{-1}))\cdot s_w \\ (1-(\sin^{-1}(\frac{z}{||c||})+f_{vup})\cdot f_v^{-1})\cdot s_h \end{bmatrix} \tag{1}$$

The dimensions of the projected image are defined by s_h (height) and s_w (width), with f_v representing the sensor's total vertical field of view and f_{vup} denoting the upper portion of this FOV measured from the horizontal reference plane. These parameters generate image coordinates that form a three-channel (x, y, z) representation of the structured point cloud $P_o \in \mathbb{R}^{s_h \times s_w \times (3+C_f)}$, where C_f corresponds to supplementary feature dimensions.

2.2 Spatial Branch

Traditional filter-based point cloud denoising methods primarily design filter algorithms based on certain a priori knowledge, such as noise points being isolated, LiDAR-acquired point clouds being denser near the sensor and sparser farther away (J. Yu et al., 2025), and the disordered nature of snowflake noise points. However, these methods have limitations in handling complex environments, particularly in removing noise points while preserving environmental features. Inspired by the strategy in 4DenoiseNet (Seppanen et al., 2023), we introduced a convolution operation based on kNN in the first layer of the network to enhance the neural network's ability to capture local spatial information. Unlike traditional convolution kernels based on pixel coordinates, kNN-convolution selects the k nearest neighbors of each point in metric space. This method enables better distinction of dynamic noise points, as illustrated in Fig. 1. Since performing kNN searches directly across the entire point cloud is computationally expensive, we limit the search to the local region around each point, thereby reducing computational complexity. In the current point cloud frame P(t), the kNN algorithm searches for the k nearest neighbors of each point. The search results are unfolded to generate neighborhood features, as described by the following equation:

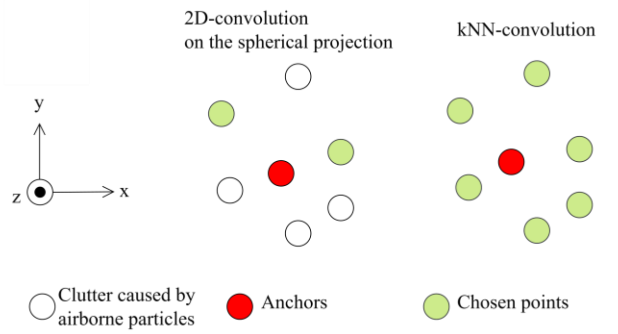

Figure 1. Comparison of 2D convolution and kNN-convolution in distinguishing dynamic noise points and capturing local spatial features.

$$k_s(p) = w * P_o^{(t)} = \sum_{\partial p=0}^{k} w(\partial p) \cdot P_o^{(t)}(\psi(p))(\partial p) \tag{2}$$

Where w represents the weight of the trainable convolutional kernel, and $\psi(p)$ is the index function used to select the k nearest points from the neighboring points, defined as:

$$\psi(p) = argmink(|P_{or}^{(t)}(p-\xi, \ldots, p+\xi) - P_{or}^{(t)}(p)|) \tag{3}$$

Where, $P_{or}^{(t)}$ denotes the range channel, and ξ is a hyperparameter for the search range.

2.3 Temporal Branch

In LiDAR point clouds, snowflake noise points typically exhibit more chaotic characteristics compared to environmental features. This is due to the reflection of laser beams by airborne particles. Unlike the reflections from static surfaces, the reflections from snowflakes are more random, and this randomness is manifested as dynamic changes in the point cloud data. Studies show that reflections caused by snow are almost never found in the same position between adjacent scans, whereas reflections from static surfaces exhibit higher temporal consistency. Based on this observation and the strategy in 4DenoiseNet (Seppanen et al., 2023), we introduce temporal information into point cloud denoising by performing contrastive analysis between adjacent frames, which effectively distinguishes dynamic noise points from static non-noise points. As shown in Fig. 2, we capture temporal information by searching the kNN set from the previous frame's point cloud P(t−1), with the current frame's anchor point $a \in \mathbb{R}^{s_h \times s_w \times 3}$ as a reference. These anchor points correspond to the Cartesian coordinate channels of the current point cloud frame P(t). Similar to the spatial kNN search in P(t), the temporal kNN search is also conducted within the local neighborhood of the ordered point cloud.
The kNN-convolution of the temporal branch is defined as:

$$k_t(p) = w_\Delta * d = \sum_{\partial p=0}^{k} w_\Delta(\partial p) \cdot (a(p) - P_o^{(t-1)}(\psi_\Delta(p)))(\partial p) \tag{4}$$

Where $\psi_\Delta(p)$ is defined as:

$$\psi_\Delta(p) = argmink(|P_{or}^{(t-1)}(p-\xi, \ldots, p+\xi) - P_{or}^{(t)}(p)|) \tag{5}$$

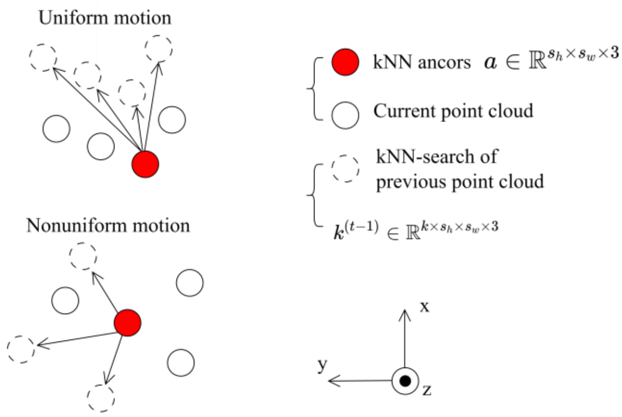

Figure 2. The Temporal-kNN-kernel capturing temporal information.

2.4 SnowSTNet Design

The network architecture of SnowSTNet is shown in Fig. 3. The network consists of two branches: the spatial branch processes the spatial features of the current frame's point cloud P(t), and the temporal branch processes the temporal features of the previous frame's point cloud P(t−1). The spatial branch contains kNN-convolution blocks that capture the kNN of each point. The temporal branch also performs kNN search, but the anchor points are provided by the spatial branch and are subtracted from the kNN points of the previous point cloud P(t−1). To further enhance feature fusion across time, we follow the design idea of MF-MOS (Cheng et al., 2024), where the two branches are connected through multiple MGA blocks. The encoded features from the previous frame's point cloud are combined with the features of each layer of the current frame's point cloud and passed as input to the subsequent encoding modules of the temporal branch.
The feature fusion process can be expressed as:

$$F_s = sigmoid(Conv_{1\times1}(F_{spatial})) \otimes F_{temporal} \tag{6}$$

The equations represents that the range image feature $F_{spatial}$ is passed through a 1×1 convolution to generate the spatial attention weight map, which is then activated by a sigmoid function to constrain the weights within the range of [0, 1]. Subsequently, the weight map is element-wise multiplied with the residual image feature $F_{temporal}$ to obtain the fused spatial attention feature F_s. This process effectively highlights important spatial regions and suppresses background noise.

$$F_c = softmax(Conv_{1\times1}(Pool(F_s))) \times C \tag{7}$$

The equations define the channel attention mechanism. Global average pooling is first applied to F_s, which is passed through a 1×1 convolution and softmax to generate channel-wise weights. These weights modulate the spatial attention features, producing the fused feature F_c. Finally, a residual connection adds the original input to the weighted features.

$$F_{final} = F_c + F_{spatial} \tag{8}$$

We adjusted the channel-to-image aspect ratio in the PixelShuffle operation of the encoder to match the modified rectangular pooling operation.

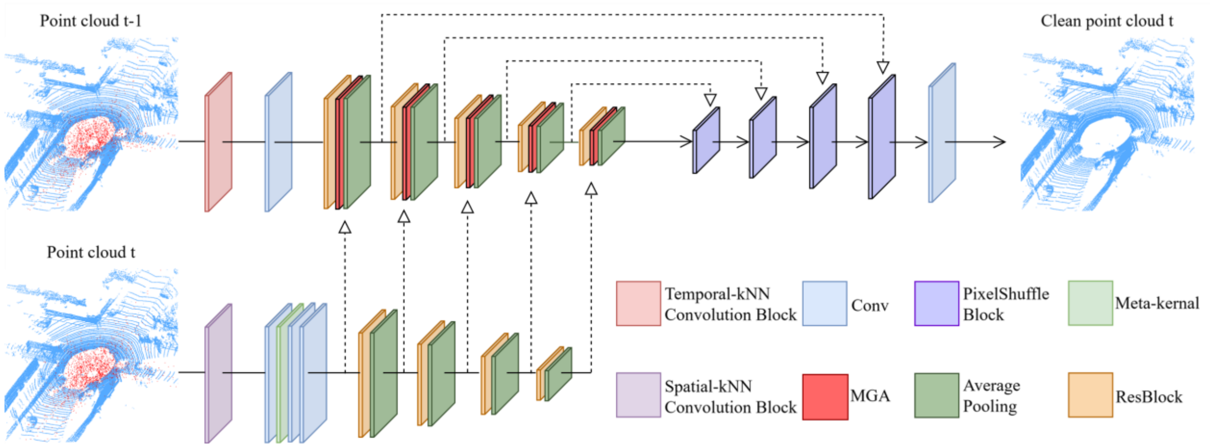

Figure 3. Architecture of our proposed SnowSTNet.

3. Experiments

3.1 Datasets

In the experiments of this study, we used a publicly available adverse weather point cloud dataset—the SnowyKITTI dataset with snow labels. This dataset consists of snow-affected LiDAR point cloud data generated by a snowfall simulation algorithm. We classified the adverse weather in the dataset based on different snowfall rates. Additionally, we divided the dataset into three parts: training set, validation set, and test set. The specific details of the dataset split are shown in Table 1.

Classification	Light	Medium	Heavy
Snowfall Rate	[0.5, 1.5)	[1.5, 2.5)	[2.5, 3.0]
Number of Frames	20546	10539	12467
Train Valid Test	0,2,19 17,18 8	1,5,9,10 3,4,20 11,12	6,13,15,21 16 7,14

Table 1. Split of the Adverse Weather Dataset under Snowfall

3.2 Comparison with the State-of-the-art Methods

In the quantitative experiments, we use Mean Intersection-over-Union (MIoU) as the evaluation metric:

$$\mathrm{IoU}_i = \frac{TP_i}{TP_i + FP_i + FN_i} \tag{9}$$

$$\mathrm{MIoU} = \sum_{i=1}^{cls} \mathrm{IoU}_i \tag{10}$$

Where TP_i FP_i FN_i represent the number of true positives, false positives, and false negatives for the i-th class, respectively. The overall mean IoU (mIoU) is computed by averaging the class-wise IoUs across all categories.
We conducted denoising experiments under snowy weather to compare SnowSTNet with state-of-the-art (SOTA) methods. The quantitative results, presented in Table 2, include IoU for individual categories, MIoU across all categories, as well as the average runtime and number of parameters. Some baseline results, such as those for AdverseNet (Yan et al., 2025), are directly adopted from their original publication. The comparison includes deep learning-based and filter-based methods. In comparison to these methods, the results indicate that SnowSTNet achieves the highest IoU and MIoU across the Light Snow, Medium Snow, Heavy Snow, and Clear categories.

Method	Light Snow IoU (%)	Medium Snow IoU (%)	Heavy Snow IoU (%)	Clear IoU (%)	MIoU (%)	Average Runtime (ms)	Parameters
SOR	10.36	12.23	14.42	85.46	30.62	70.41	2
ROR	10.70	15.23	20.73	93.46	35.03	67.02	2
DSOR	67.00	67.02	63.88	98.68	74.15	61.44	3
DROR	54.00	59.44	59.84	98.27	67.89	110.48	4
LiSnowNet	40.16	25.10	18.18	97.76	45.30	2.44	1.4M
4DenoiseNet	96.21	95.74	95.05	99.90	96.73	34.03	0.6M
SnowSTNet	97.73	95.99	95.11	99.92	97.19	32.84	2.6M

Table 2. Quantitative Results of Denoising Experiments in Snowy weather

Through Table 2, we observe that the MIoU of SOR and ROR is lower than that of DSOR and DROR, which indicates that DSOR and DROR, as improvements over SOR and ROR, effectively leverage the prior knowledge that LiDAR point clouds exhibit higher density at close range and sparser distribution at greater distances. As deep learning-based comparison methods, LiSnowNet and 4DenoiseNet prioritize lightweight design, and thus use distance views to represent the point cloud in the network. This approach allows them to learn complex noise features, resulting in generally higher MIoU compared to filter-based methods. However, LiSnowNet performs poorly in snow denoising experiments, mainly because it relies on a set of complex threshold hyperparameters to achieve higher algorithm efficiency. While LiSnowNet's Average Runtime is significantly lower than that of other methods in snow denoising experiments, its reliance on threshold hyperparameters is not adaptable to the varying snowfall rates of Light Snow, Medium Snow, and Heavy Snow, leading to poor performance. Our proposed SnowSTNet achieves the highest IoU and MIoU across different levels of snowfall, with an average runtime slightly shorter than that of the similarly performing 4DenoiseNet. This demonstrates that SnowSTNet effectively learns complex noise features under snowy weather.

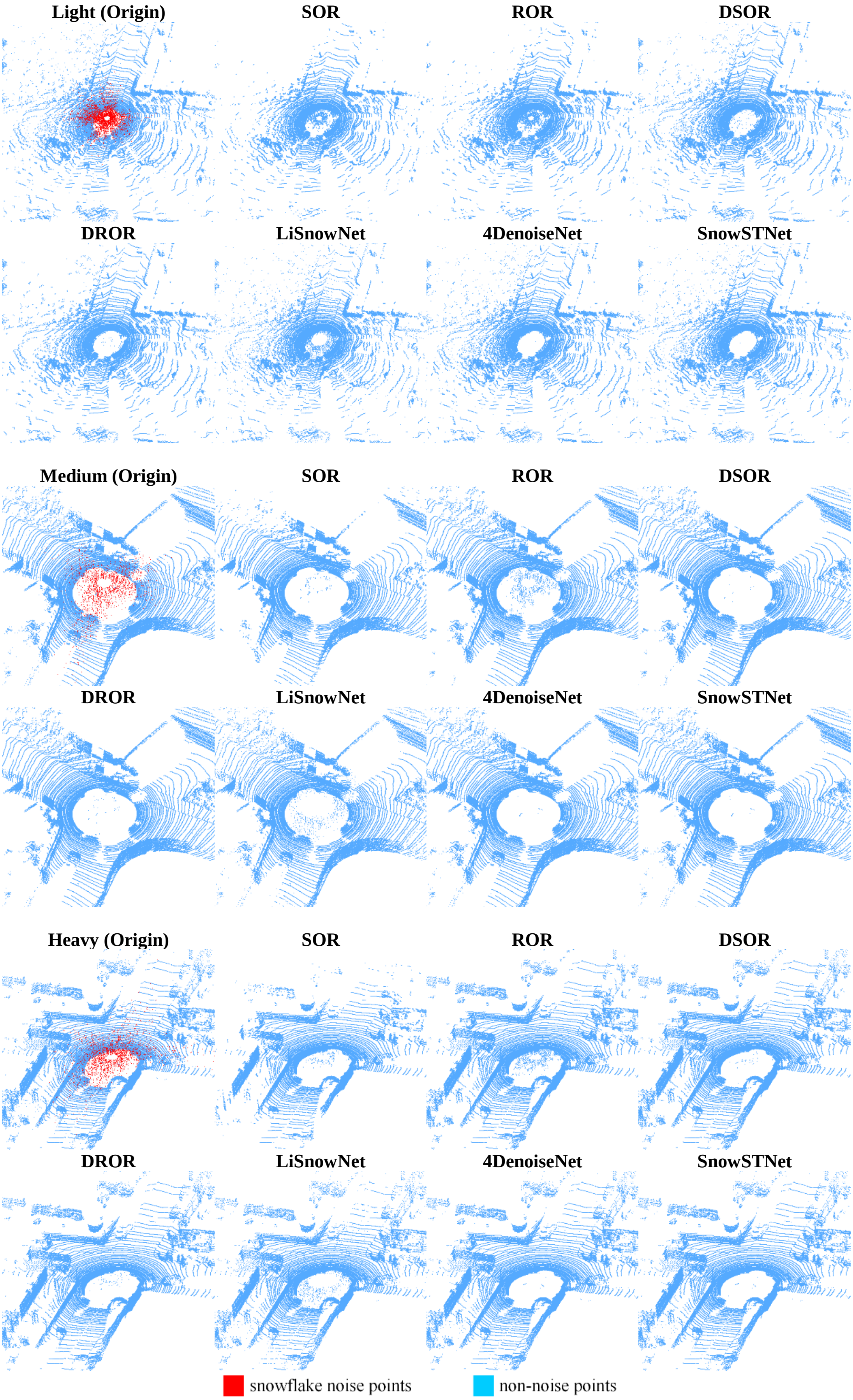

Figure 4. Visualization of denoising results for snowy weather.

We present the qualitative results of the denoising comparison experiments under snowy weather, as shown in Figure 4. For the sake of comparison, we display the original point clouds from three different levels of snowfall, as well as the denoised results for each method. The blue points represent non-noise points, while the red points represent snowflake noise points. Observing the denoising results of SOR and ROR, we find that both leave a large number of noise points unremoved, but ROR has a better ability to retain environmental features compared to SOR. Upon examining the denoising results of DSOR, we observe that its performance is better for medium snow and heavy snow compared to light snow. This reveals a drawback of the DSOR method: it cannot achieve consistent denoising performance across point clouds with different snowfall rates using the same set of parameters. In contrast, DROR exhibits roughly similar denoising performance across all three snowfall rates, indicating that DROR is more robust to point clouds with varying degrees of snowfall. LiSnowNet generates denoised results with substantial residual noise, and its performance falls behind DSOR and DROR. This indicates that setting too many threshold hyperparameters, while shortening the model's average runtime, also limits the advantage of deep learning over traditional filter parameter settings, making it unable to automatically adjust the threshold hyperparameters according to different snowfall rates. 4DenoiseNet effectively removes almost all the noise points, achieving excellent denoising performance. Our proposed SnowSTNet achieves a slight improvement over 4DenoiseNet. Since both methods already achieve near-perfect denoising, further improvements in accuracy become increasingly challenging. Overall, the denoising results demonstrate that SnowSTNet performs well across different snowfall rates.

3.3 Ablation Study

To assess the contribution of the spatial-temporal kNN-convolution and MGA blocks, we performed ablation experiments on four modified versions of SnowSTNet. Table III summarizes their IoU performance, inference time, and parameter count. This study examines the effects of using traditional 2D convolution layers versus kNN-convolution modules, as well as the impact of incorporating multiple MGA blocks.

The results in Table III highlight the influence of different convolution types and the use of MGA blocks on model performance and computational efficiency. When using 2D convolution without MGA, the model achieves IoU scores of 95.99%, 94.38%, and 93.65% for Light Snow, Medium Snow, and Heavy Snow, respectively, while maintaining the shortest runtime (21.69 ms). Introducing MGA within the 2D convolution framework provides a slight improvement in Light and Medium Snow IoU (+0.39% and +0.11%, respectively) but has a negligible effect on Heavy Snow (-0.11%), with an almost unchanged runtime.

In contrast, replacing 2D convolution with kNN-convolution significantly enhances model performance across all snowfall rates. Without MGA, kNN-convolution improves IoU scores for Light, Medium, and Heavy Snow by +1.45%, +1.24%, and +1.37%, respectively, compared to the baseline 2D convolution model. However, this performance gain comes at the cost of increased runtime (31.92 ms vs. 21.69 ms). When MGA is integrated with kNN-convolution, the model achieves the highest IoU across all categories (97.73%, 95.99%, and 95.11%), demonstrating that the combination of kNN-convolution and multiple MGA blocks yields the best overall performance. Nevertheless, this configuration also results in the highest computational cost, with the longest runtime (32.84 ms), highlighting the trade-off between performance and efficiency.

These findings suggest that while kNN-convolution outperforms 2D convolution in denoising under Snowfall, incorporating multiple MGA blocks further enhances performance, particularly in Light and Medium Snow. However, the increased computational overhead must be considered for real-time applications.

First conv	MGA	Light IoU(%)	Medium IoU(%)	Heavy IoU(%)	Runtime (ms)	Parameters
2D	-	95.99	94.38	93.65	21.69	2.6M
2D	✓	96.38	94.49	93.54	21.79	2.6M
kNN	-	97.44	95.62	95.02	31.92	2.6M
kNN	✓	97.73	95.99	95.11	32.84	2.6M

Table 3. Ablation Study on the Performance Impact of Different Modules

4. Conclusion

This paper proposes a novel point cloud denoising network, SnowSTNet, aimed at addressing the noise issues in LiDAR point cloud data under snowy weather. By adopting a dual-branch architecture that processes spatial and temporal information simultaneously, SnowSTNet effectively removes snowflake noise points and restores more accurate environmental details. Experimental results show that, compared to other methods, SnowSTNet achieves the highest accuracy in both MIoU and IoU metrics, consistently delivering excellent denoising performance across various snowfall rates. By improving LiDAR perception capabilities, SnowSTNet enables more reliable environmental understanding for autonomous vehicles, thereby enhancing system robustness and deployment in adverse weather.

References

Bae, G., Kim, B., Ahn, S., Min, J., & Shim, I. (2022). SLiDE: Self-supervised LiDAR De-snowing Through Reconstruction Difficulty. Computer Vision – ECCV 2022, 283–300. https://doi.org/10.1007/978-3-031-19842-7_17

Balta, H., Velagic, J., Bosschaerts, W., De Cubber, G., & Siciliano, B. (2018). Fast Statistical Outlier Removal Based Method for Large 3D Point Clouds of Outdoor Environments. IFAC-PapersOnLine, 51(22), 348–353. https://doi.org/10.1016/j.ifacol.2018.11.566

Charron, N., Phillips, S., & Waslander, S. L. (2018). De-noising of Lidar Point Clouds Corrupted by Snowfall. 2018 15th Conference on Computer and Robot Vision (CRV), 254–261. https://doi.org/10.1109/CRV.2018.00043

Cheng, J., Zeng, K., Huang, Z., Tang, X., Wu, J., Zhang, C., Chen, X., & Fan, R. (2024). MF-MOS: A Motion-Focused Model for Moving Object Segmentation (arXiv:2401.17023). arXiv. https://doi.org/10.48550/arXiv.2401.17023

Cortinhal, T., Tzelepis, G., & Erdal Aksoy, E. (2020). SalsaNext: Fast, Uncertainty-Aware Semantic Segmentation of LiDAR Point Clouds. In G. Bebis, Z. Yin, E. Kim, J. Bender, K. Subr, B. C. Kwon, J. Zhao, D. Kalkofen, & G. Baciu (Eds.), Advances in Visual Computing (pp. 207–222). Springer International Publishing. https://doi.org/10.1007/978-3-030-64559-5_16

Duan, Y., Yang, C., Chen, H., Yan, W., & Li, H. (2021). Low-complexity point cloud denoising for LiDAR by PCA-based dimension reduction. Optics Communications, 482, 1 26567. https://doi.org/10.1016/j.optcom.2020.126567

Duan, Y., Yang, C., & Li, H. (2021). Low-complexity ada ptive radius outlier removal filter based on PCA for lidar point cloud denoising. Applied Optics, 60(20), E1. https://d oi.org/10.1364/AO.416341

Heinzler, R., Piewak, F., Schindler, P., & Stork, W. (2020). CNN-Based Lidar Point Cloud De-Noising in Adverse We ather. IEEE Robotics and Automation Letters, 5(2), 2514–2 521. https://doi.org/10.1109/LRA.2020.2972865

Huang, H., Yan, X., Yang, J., Cao, Y., & Zhang, X. (202 3). LIDSOR: A FILTER FOR REMOVING RAIN AND S NOW NOISE POINTS FROM LIDAR POINT CLOUDS I N RAINY AND SNOWY WEATHER. The International A rchives of the Photogrammetry, Remote Sensing and Spatia l Information Sciences, XLVIII-1/W2-2023, 733–740. https:/ /doi.org/10.5194/isprs-archives-XLVIII-1-W2-2023-733-2023

Kurup, A., & Bos, J. (2021). DSOR: A Scalable Statistical Filter for Removing Falling Snow from LiDAR Point Clo uds in Severe Winter Weather (arXiv:2109.07078). arXiv. h ttp://arxiv.org/abs/2109.07078

Luo, Z., Ma, J., Xiong, G., Hu, X., Zhou, Z., & Xu, J. (2 022). Semantic Segmentation Based Rain and Fog Filtering Only by LiDAR Point Clouds. 2022 IEEE International C onference on Unmanned Systems (ICUS), 90–95. https://doi. org/10.1109/ICUS55513.2022.9986567

Park, J.-I., Park, J., & Kim, K.-S. (2020). Fast and Accura te Desnowing Algorithm for LiDAR Point Clouds. IEEE A ccess, 8, 160202–160212. https://doi.org/10.1109/ACCESS.20 20.3020266

Piewak, F., Pinggera, P., Schäfer, M., Peter, D., Schwarz, B., Schneider, N., Enzweiler, M., Pfeiffer, D., & Zöllner, M. (2019). Boosting LiDAR-Based Semantic Labeling by Cross-modal Training Data Generation. In L. Leal-Taixé & S. Roth (Eds.), Computer Vision – ECCV 2018 Workshops (Vol. 11134, pp. 497–513). Springer International Publishin g. https://doi.org/10.1007/978-3-030-11024-6_39

Qu, C., Zhang, Y., Sun, Z., Ma, F., & Zhang, X. (2024). Point Clouds Denoising Method Based on SPAD Discrete Probability Model and Completion. IEEE Transactions on Geoscience and Remote Sensing, 62, 1–15.

Roriz, R., Campos, A., Pinto, S., & Gomes, T. (2022). DI OR: A Hardware-Assisted Weather Denoising Solution for LiDAR Point Clouds. IEEE Sensors Journal, 22(2), 1621–1 628. https://doi.org/10.1109/JSEN.2021.3133873

Rusu, R. B., & Cousins, S. (2011). 3D is here: Point Clou d Library (PCL). 2011 IEEE International Conference on R obotics and Automation, 1–4. https://doi.org/10.1109/ICRA.2 011.5980567

Seppanen, A., Ojala, R., & Tammi, K. (2023). 4DenoiseNe t: Adverse Weather Denoising From Adjacent Point Clouds. IEEE Robotics and Automation Letters, 8(1), 456–463. htt ps://doi.org/10.1109/LRA.2022.3227863

Wang, W., You, X., Chen, L., Tian, J., Tang, F., & Zhang, L. (2022). A Scalable and Accurate De-Snowing Algorith m for LiDAR Point Clouds in Winter. Remote Sensing, 14 (6), 1468. https://doi.org/10.3390/rs14061468

Yan, X., Yang, J., Liang, Y., Ma, Y., Li, Y., & Huang, H. (2025). AdverseNet: A LiDAR Point Cloud Denoising Net work for Autonomous Driving in Rainy, Snowy, and Foggy Weather. IEEE Sensors Journal, 25(5), 8950–8961. https:// doi.org/10.1109/JSEN.2024.3505234

Yan, X., Yang, J., Zhu, X., Liang, Y., & Huang, H. (202 4). Denoising Framework Based on Multiframe Continuous Point Clouds for Autonomous Driving LiDAR in Snowy Weather. IEEE Sensors Journal, 24(7), 10515–10527. https:/ /doi.org/10.1109/JSEN.2024.3358341

Yu, J., Huang, A., Sun, Z., Huang, R., Huang, G., & Zha o, Q. (2025). Loss Function Optimization Method and Uns upervised Extraction Approach D-DBSCAN for Improving t he Moving Target Perception of 3D Imaging Sonar. Journal of Marine Science and Engineering, 13(3), 529.

Yu, M.-Y., Vasudevan, R., & Johnson-Roberson, M. (2022). LiSnowNet: Real-time Snow Removal for LiDAR Point C louds. 2022 IEEE/RSJ International Conference on Intellige nt Robots and Systems (IROS), 6820–6826. https://doi.org/1 0.1109/IROS47612.2022.9982248